A Kernel-Based Time-Stepping Framework for Stiff PDEs: Revisiting MOLT with SSP-RK

Sining Gong
Michigan State University

Joint work with Hyoseon Yang (Kyung Hee University), Andrew Christlieb (MSU)

Innovative and Efficient Strategies for Stiff Differential Equations @ ICERM

Thanks to DOE-CHaRMNET and MURI for funding this work

Contents

Motivations

- Stiff PDEs often require implicit time-stepping methods
  - IMEX, fully implicit...
- Method line of transpose (MOL^T) or Rothe's method uses Kernel-based operators in combined with explicit SSP-RK to retain unconditionally stability.
- Compared with Method of Line (MOL): $O(N)$-linear computational cost without calculating inverse of a matrix - efficiency
  - IVP to BVP
- Such a method can be viewed as a Kernel-based time-stepping framework which is expected to be applied to many types of PDEs including stiff PDEs.

Kernel-based representation of ∂_x and ∂_{xx}

- The kernel-based representation of the first spatial derivative ∂_x and second spatial derivative ∂_{xx}. (A. Christlieb, Guo, et al., 2020; Causley and A. J. Christlieb, 2014)

Let us consider this problem:

$$u_t + f(u)_x = g(u)_{xx}, \qquad x \in [a, b] \tag{1}$$

where $g'(u) \geq 0$ and $g'(u)$ can vanish for some values of u.

- To derive two operators to discretize ∂_x and ∂_{xx}, solve the equation with explicit SSP-RK (unconditionally stable).

Kernel-based representation of ∂_x and ∂_{xx}

- The kernel-based representation of the first spatial derivative ∂_x and second spatial derivative ∂_{xx}. (A. Christlieb, Guo, et al., 2020; Causley and A. J. Christlieb, 2014)
- Considering a hyperbolic conservation law:

$$\partial_t u + (cu)_x = 0, \quad x \in [a, b]. \tag{2}$$

Using the backward Euler time discretization, we obtain

$$(1 - c\Delta t \partial_x) u^{n+1} = u^n \tag{3}$$

where $u^n := u(t^n)$ and $u^{n+1} := u(t^{n+1})$ with $\alpha := \frac{1}{c\Delta t}$

- Account for waves traveling in opposite directions, downwinding and upwinding, two function operators $\mathcal{L}_L$ and $\mathcal{L}_R$:

$$\mathcal{L}_L = \mathcal{I} - \frac{1}{\alpha}\partial_x, \quad \mathcal{L}_R = \mathcal{I} + \frac{1}{\alpha}\partial_x, \quad x \in [a, b], \tag{4}$$

Kernel-based representation of ∂_x and ∂_{xx}

- The kernel-based representation of the first spatial derivative ∂_x and second spatial derivative ∂_{xx}. (A. Christlieb, Guo, et al., 2020; Causley and A. J. Christlieb, 2014)
- The inversion of these operators:

$$\begin{aligned} \mathcal{L}_L^{-1}[v](x) &= I_L[v](x) + B_L e^{-\alpha(b-x)}, \\ \mathcal{L}_R^{-1}[v](x) &= I_R[v](x) + A_R e^{-\alpha(x-a)}, \end{aligned} \tag{5}$$

Here I_L and I_R are the integral operators given by

$$\begin{aligned} I_L[v](x) &= \alpha \int_x^b e^{-\alpha(s-x)} v(s)\, ds, \\ I_R[v](x) &= \alpha \int_a^x e^{-\alpha(x-s)} v(s)\, ds, \end{aligned} \tag{6}$$

and A_R and B_L are the constants determined by the boundary conditions.

Kernel-based representation of ∂_x and ∂_{xx}

Then we introduce the operators

$$\mathcal{D}_L = \mathcal{I} - \mathcal{L}_L^{-1}, \quad \mathcal{D}_R = \mathcal{I} - \mathcal{L}_R^{-1}, \quad x \in [a, b]. \tag{7}$$

Each of these can be expanded in a Neumann series:

$$\begin{aligned} \frac{1}{\alpha}\partial_x^+ &= \mathcal{I} - \mathcal{L}_L = \mathcal{L}_L(\mathcal{L}_L^{-1} - \mathcal{I}) = -\mathcal{D}_L/(\mathcal{I} - \mathcal{D}_L) = -\sum_{p=1}^{\infty} \mathcal{D}_L^p, \\ \frac{1}{\alpha}\partial_x^- &= \mathcal{L}_R - \mathcal{I} = \mathcal{L}_R(\mathcal{I} - \mathcal{L}_R^{-1}) = \mathcal{D}_R/(\mathcal{I} - \mathcal{D}_R) = \sum_{p=1}^{\infty} \mathcal{D}_R^p. \end{aligned} \tag{8}$$

Here ∂_x^+ and ∂_x^- indicate the left-sided and right-sided approximations of the derivative in x, respectively, along an interface.

Kernel-based representation of ∂_x and ∂_{xx}

- "flux splitting" - **Lax–Friedrichs flux**: $f^{\pm} = \frac{1}{2}(f(u) \pm cu)$, with $c = \max_u |f'(u)|$.
- $-f(u)_x$ can be represented as:

$$-\alpha_L \sum_{p=1}^{\infty} \mathcal{D}_L^p[f^+(u), \alpha_L] + \alpha_R \sum_{p=1}^{\infty} \mathcal{D}_R^p[f^-(u), \alpha_R].$$

Kernel-based representation of ∂_x and ∂_{xx}

Similarly, considering the linear heat equation

$$\partial_t v - c^2 \partial_{xx} v = 0, \quad x \in [a, b]. \tag{9}$$

Using the backward Euler time discretization and the Neumann series, we have the following operators to derive the approximation of ∂_{xx}:

$$\mathcal{L}_0 = \mathcal{I} - \frac{1}{\alpha^2}\partial_{xx}, \quad \mathcal{D}_0 = \mathcal{I} - \mathcal{L}_0^{-1}, \quad \frac{1}{\alpha^2}\partial_{xx} = -\sum_{p=1}^{\infty} \mathcal{D}_0^p, \quad x \in [a, b],$$

where $\mathcal{I}$ is an identity operator and $\alpha := \frac{1}{c\sqrt{\Delta t}}$. By doing integration by parts twice, we can have the following:

$$\mathcal{L}_0^{-1}[v^n](x) = \frac{\alpha}{2} \int_a^b e^{-\alpha|y-x|} v^n(y) dy + B_0 e^{-\alpha(b-x)} + A_0 e^{-\alpha(x-a)}, \tag{10}$$

Kernel-based representation of ∂_x and ∂_{xx}

- $-f(u)_x + g(u)_{xx}$ can be represented as:

$$-\alpha_L \sum_{p=1}^{\infty} \mathcal{D}_L^p[f^+(u), \alpha_L] + \alpha_R \sum_{p=1}^{\infty} \mathcal{D}_R^p[f^-(u), \alpha_R] - \alpha_0 \sum_{p=1}^{\infty} \mathcal{D}_0^p[g(u), \alpha_0]$$

- For different order of accuracy we need, truncate this infinite partial sum & corresponding SSP-RK
  - $\mathcal{H}[u^n] := -\alpha_L \sum_{p=1}^{k} \mathcal{D}_L^p[f^+(u^n), \alpha_L] + \alpha_R \sum_{p=1}^{k} \mathcal{D}_R^p[f^-(u^n), \alpha_R] - \alpha_0 \sum_{p=1}^{k} \mathcal{D}_0^p[g(u^n), \alpha_0]$
  - For example, the second order SSP-RK:

$$u^{(1)} = u^n + \Delta t \mathcal{H}[u^n], \tag{11}$$

$$u^{n+1} = \frac{1}{2}u^n + \frac{1}{2}(u^{(1)} + \Delta t \mathcal{H}(u^{(1)}) \tag{12}$$

Kernel-based representation of ∂_x and ∂_{xx}

(A. Christlieb, Guo, et al., 2020) Suppose $v(x)$ is a periodic smooth function.

1. Consider the operator $\mathcal{D}_0$ with the boundary treatment $\mathcal{D}_0(a) = \mathcal{D}_0(b)$. If $v(x) \in C^{2k+2}[a, b]$, then we have

$$\left\| \partial_{xx} v(x) + \alpha_0^2 \sum_{p=1}^{k} \mathcal{D}_0^p[v, \alpha_0](x) \right\|_\infty \leq C \left(\frac{1}{\alpha_0} \right)^{2k} \left\| \partial_x^{2k+2} v(x) \right\|_\infty$$

   where C is a constant only depending on k.

2. Consider the operators $\mathcal{D}_L$ and $\mathcal{D}_R$ with the boundary treatment $\mathcal{D}_L(a) = \mathcal{D}_L(b)$ and $\mathcal{D}_R(a) = \mathcal{D}_R(b)$, respectively. If $v(x) \in C^{k+1}[a, b]$, then we have

$$\left\| \partial_x v(x) - \alpha_L \sum_{p=1}^{k} \mathcal{D}_L^p[v, \alpha_L](x) \right\|_\infty \leq C \left(\frac{1}{\alpha_L} \right)^{k} \left\| \partial_x^{k+1} v \right\|_\infty,$$

   where C is a constant depending only on k and similarly for $\mathcal{D}_R$.

Stability analysis: $\alpha_0 = \frac{\sqrt{\beta}}{\sqrt{q\Delta t}}$ and $\alpha_{LR} = \frac{\beta}{c\Delta t}$

k	$\beta_{1,k,\max}$	$\beta_{2,k,\max}$	$\beta_{k,\max}$
1	2	2	1
2	1	1	0.5
3	1.243	0.8375	0.4167

Theorem

(a) *For the linear advection equation $u_t + cu_x = 0$ with periodic boundary conditions, there exists constant $\beta_{1,k,\max} > 0$ for $k = 1, 2$, such that the scheme is A-stable provided $0 < \beta \leq \beta_{1,k,\max}$.*

(b) *For the linear diffusion equation $u_t = qu_{xx}$ with $q > 0$ and periodic boundary conditions, there exists constant $\beta_{2,k,\max} > 0$ for $k = 1, 2, 3$, such that the scheme is A-stable provided $0 < \beta \leq \beta_{2,k,\max}$.*

The constants $\beta_{1,k,\max}$ and $\beta_{2,k,\max}$ are summarized in Table.

Stability analysis: Sketch of proof

(a) For $c > 0$, Upon the definitions of $\mathcal{D}_L$ and $\mathcal{L}_L$, by taking the Fourier transform in space, we obtain that

$$\widehat{\mathcal{L}}_L = 1 + (i\kappa)/\alpha_L,$$

and then

$$\widehat{\mathcal{D}}_L = 1 - 1/\widehat{\mathcal{L}}_L = \frac{i\kappa/\alpha_L}{1 + i\kappa/\alpha_L}.$$

For the forward Euler scheme

$$u^{n+1} = u^n - \Delta t\, \alpha_L\, \mathcal{D}_L[cu^n, \alpha_L],$$

with the parameter $\alpha_L = \beta/(c\Delta t)$, we could compute the amplification factor λ

$$\lambda = 1 - \beta\, \frac{i\kappa c\Delta t/\beta}{1 + i\kappa c\Delta t/\beta}.$$

Then, we have $|\lambda| \leq 1$ when $\beta \leq 2$, which implies the scheme is A-stable. Hence, for the first order scheme $k = 1$, we can choose $\beta_{1,1,\max} = 2$.

Stability analysis: Sketch of proof

(b) Similarly, for the forward Euler scheme

$$u^{n+1} = u^n - \Delta t\, \alpha_0\, \mathcal{D}_0[qu^n, \alpha_0],$$

and $\alpha_0 = \sqrt{\beta}/(q\Delta t)$, the amplification factor λ is

$$\lambda = 1 - \beta\widehat{\mathcal{D}}_0 \quad \text{with} \quad \widehat{\mathcal{D}}_0 = 1 - 1/\widehat{\mathcal{L}}_0 = \frac{(\kappa/\alpha_0)^2}{1 + (\kappa/\alpha_0)^2} \in [0, 1].$$

Then, we still have $\beta \leq 2$ to ensure $|\lambda| \leq 1$. Thus, we let $\beta_{2,1,\max} = 2$.

Short summary of the base scheme

1. Determine the parameters β.
2. On each inner stage of the k^{th} order SSP RK scheme:
   1. Compute c, q at each time level t^n, and then obtain parameters $\alpha_0, \alpha_L, \alpha_R$
      1. Split $f(u)$ into $f^{\pm}(u)$.
      2. Apply $\mathcal{D}_L$ and $\mathcal{D}_R$ on f^+ and f^-, respectively. Use the WENO quadrature to calculate $I^{L,R}$, combined with A_L and B_R to construct $\mathcal{D}_L[f^+]$ and $\mathcal{D}_R[f^-]$.
      3. For $k > 1$, further construct

$$\mathcal{D}_L^p[f^+] = \mathcal{D}_L^{p-1}[\mathcal{D}_L[f^+]], \quad \mathcal{D}_R^p[f^-] = \mathcal{D}_R^{p-1}[\mathcal{D}_R[f^-]]$$

      by a similar procedure for $1 < p \leq k$. WENO quadrature is not needed for construction of these high order terms.
   2. Diffusion part: follow a similar procedure to construct the partial sum approximation to $g(u)_{xx}$ using operator $\mathcal{D}_0$.
   3. Substitute the partial sum approximations and update the solution accordingly.

Periodic boundary with Stiff case - by my collaborators

- Boundary terms: $A_L = \frac{I_L[v](b)}{1-\mu}$, $B_R = \frac{I_R[v](a)}{1-\mu}$, $A_0 = \frac{I_0[v](b)}{1-\mu}$, $B_0 = \frac{I_0[v](a)}{1-\mu}$.
- We consider this problem (A. Christlieb, Guo, et al., 2020):

$$\begin{cases} u_t + c\,u_x = q\,u_{xx}, \ -\pi \le x \le \pi, \\ u(x,0) = \sin(x), \end{cases}$$

with the 2π-periodic boundary condition. Here, c and $q \ge 0$ are given constants. This problem has the exact solution $u^e(x,t) = e^{-qt}\sin(x-ct)$. Given $c = 1$ and $q = 0.01$.

Periodic boundary with Stiff case

CFL	N_x	$k = 1.\ \beta = 1.$		$k = 2.\ \beta = 0.5.$		$k = 3.\ \beta = 0.4.$	
		Error	Order	Error	Order	Error	Order
0.5	40	7.260E−02	–	4.729E−02	–	2.559E−03	–
	80	3.715E−02	0.967	1.218E−02	1.957	1.712E−04	3.902
	160	1.885E−02	0.979	3.077E−03	1.985	1.091E−05	3.972
	320	9.473E−03	0.992	7.703E−04	1.998	6.865E−07	3.990
	640	4.750E−03	0.996	1.928E−04	1.999	4.357E−08	3.978
1	40	1.388E−01	–	1.697E−01	–	3.263E−02	–
	80	7.260E−02	0.935	4.729E−02	1.843	2.559E−03	3.672
	160	3.717E−02	0.966	1.218E−02	1.956	1.712E−04	3.902
	320	1.885E−02	0.980	3.077E−03	1.986	1.091E−05	3.973
	640	9.473E−03	0.992	7.703E−04	1.998	6.864E−07	3.990
2	40	2.474E−01	–	4.375E−01	–	2.313E−01	–
	80	1.388E−01	0.834	1.697E−01	1.366	3.271E−02	2.822
	160	7.260E−02	0.935	4.733E−02	1.842	2.561E−03	3.675
	320	3.717E−02	0.966	1.218E−02	1.958	1.713E−04	3.902
	640	1.885E−02	0.980	3.077E−03	1.986	1.091E−05	3.973

Homogeneous Dirichlet boundary with Stiff case

For the nonlinear case, we have

$$u_t + f(u)_x = \varepsilon(\nu(u)u_x)_x, \qquad 0 \le x \le 1 \tag{13}$$

where $f(u) = \frac{u^2}{u^2+(1-u)^2}$,

$$\nu(u) = \begin{cases} 4u(1-u), & 0 \le u \le 1 \\ 0, & \text{otherwise} \end{cases} \tag{14}$$

$$u(x,0) = \begin{cases} 0, \ 0 \le x < 1 - \frac{1}{\sqrt{2}}, \\ 1, \ 1 - \frac{1}{\sqrt{2}} \le x \le 1. \end{cases}$$

Homogeneous Dirichlet boundary with Stiff case

- Unconditionally stable - the performance may not be satisfactory when an exceedingly large CFL number is used
- Large CFL introduces too much numerical diffusion
- Without generating noticeable spurious oscillations

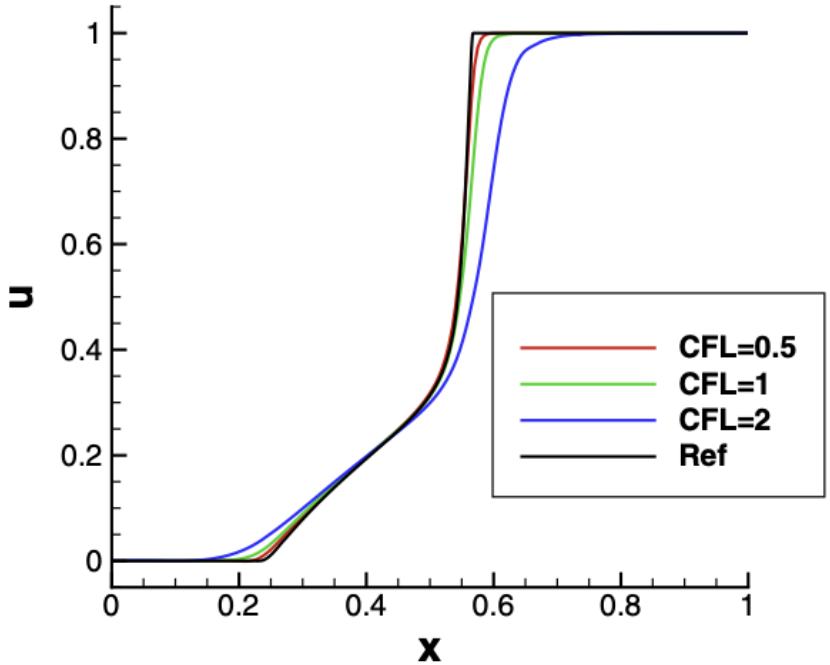

Short summary and what is next?

- (Stiff) Advection-diffusion problem with periodic and homogenous Dirichlet boundary conditions.
- Other boundary conditions? Other geometry?
- Applying to non-periodic or inhomogeneous Dirichlet boundary, high order operators lead to order reduction to the first order.
- A starting work with boundary corrections operators, unified (A. Christlieb, Gong, and Yang, 2024)

General boundary corrections

- Take $\mathcal{D}_0$ as an example. The general boundary operator is:

$$B_0 = \frac{1}{2}(v^{n+1}(b) + \frac{1}{\alpha} v_x^{n+1}(b)), \qquad A_0 = \frac{1}{2}(v^{n+1}(a) - \frac{1}{\alpha} v_x^{n+1}(a)). \tag{15}$$

- The boundary term can be approximated by Taylor expansion and the equation (9):

$$\begin{aligned} v^{n+1}(b) &= v^n(b) + (\Delta t) v_t^n(b) + \mathcal{O}(\Delta t^2) \\ &= v^n(b) + (c^2 \Delta t) v_{xx}^n(b) + \mathcal{O}(\Delta t^2) \\ &= v^n(b) + \frac{1}{\alpha^2} v_{xx}^n(b) + \mathcal{O}(\Delta t^2), \end{aligned} \tag{16}$$

and we also have similar result for $v^{n+1}(a)$.

General boundary corrections

Lemma: Suppose $v \in \mathcal{C}^{2k+2}[a,b]$ and we set the operator $\mathcal{D}_0$ with general boundary treatment (15) with (16). Then, we can obtain that

$$\begin{aligned}\mathcal{D}_0[v](x) = &-\sum_{p=1}^{k}(\frac{1}{\alpha})^{2p}\partial_x^{2p}v(x) - (\frac{1}{\alpha})^{2k+2}I_0[\partial_x^{2k+2}v](x) \\ &+\frac{1}{2}\sum_{p=4}^{2k+1}(-\frac{1}{\alpha})^{p}\partial_x^{p}v(a)e^{-\alpha(x-a)} \\ &+\frac{1}{2}\sum_{p=4}^{2k+1}(\frac{1}{\alpha})^{p}\partial_x^{p}v(b)e^{-\alpha(b-x)}.\end{aligned} \tag{17}$$

General boundary corrections

- High order approximations.

$$\widetilde{\widetilde{\mathcal{D}}}_0^p[\phi](x) = \widetilde{\mathcal{D}}_0^p[\phi](x) + \frac{1}{2}\sum_{m=p+1}^{k} c_{p,m-1}((\frac{1}{\alpha})^{2m}\partial_x^{2m}\phi(a)$$
$$+ (-\frac{1}{\alpha})^{2m+1}\partial_x^{2m+1}\phi(a))e^{-\alpha(x-a)}$$
$$+ \frac{1}{2}\sum_{m=p+1}^{k} c_{p,m-1}(\left(\frac{1}{\alpha}\right)^{2m}\partial_x^{2m}\phi(b)$$
$$+ (\frac{1}{\alpha})^{2m+1}\partial_x^{2m+1}\phi(b))e^{-\alpha(b-x)}, \quad p \geq 1,$$

$$\widetilde{\mathcal{D}}_0^p[\phi](x) = \mathcal{D}_0[\widetilde{\widetilde{\mathcal{D}}}_0^{p-1}][\phi](x), \quad p \geq 2,$$

$$c_{1,m} = -1, c_{p,m} = -\sum_{i=p-1}^{m-1} c_{p-1,i},$$

General boundary corrections

$$\phi_{xx}(x) \approx \mathcal{P}_k^0[\phi](x) = -\alpha^2 \left(\mathcal{D}_0[\phi](x) + \sum_{p=2}^{k} \widetilde{\mathcal{D}}_0^p[\phi](x) \right) \tag{18}$$

Theorem

Suppose $\phi \in \mathcal{C}^{2k+2}[a, b]$, $k = 1, 2, 3$. *Then, the modified partial sums* (18) *satisfy*

$$\|\partial_{xx}\phi(x) - \mathcal{P}_k^0[\phi](x)\|_\infty \leq C \left(\frac{1}{\alpha}\right)^{2k} \|\partial_x^{2k+2}\phi(x)\|_\infty. \tag{19}$$

Numerical results: general boundary corrections

One-dimensional heat equation example with non-homogenoues Dirichlet and Neumann boundary conditions:

$$u_t = q\, u_{xx}, \quad u(x,0) = f(x), \quad a < x < b. \tag{20}$$

Here, $q \geq 0$ is a given constant.

- Inflow Dirichlet boundary condition: Let $a = -1, b = 1$, $u(-1,t) = -e^{-\frac{1}{2}-\frac{1}{4}t}$ and $u(1,t) = e^{\frac{1}{2}-\frac{1}{4}t}$, $f(x) = (\sin(\pi x) + x)e^{0.5x}$, and then the exact solution $u^e(x,t) = e^{-\frac{1}{4}t-\pi^2 t+\frac{1}{2}x}\sin(\pi x) + xe^{\frac{1}{2}x-\frac{1}{4}t}$. The numerical test is done at final time $T = 0.5$.

- Neumann boundary condition: Let $a = 0, b = 1$, $u_x(0,t) = \pi e^{-\pi^2 t} + e^t$ and $u_x(1,t) = -\pi e^{-\pi^2 t} + e^{1+t}$, $f(x) = \sin(\pi x) + e^x$, and the exact solution $u^e(x,t) = \sin(\pi x)e^{-\pi^2 t} + e^{x+t}$. The numerical test is done at final time $T = 0.5$.

Numerical results: general boundary corrections

As shown in the figure, the use of the k-th partial sum yields k-th order accuracy, thereby verifying our theories. Moreover, the scheme allows for large CFL numbers, say CFL $= 1$ and 2.

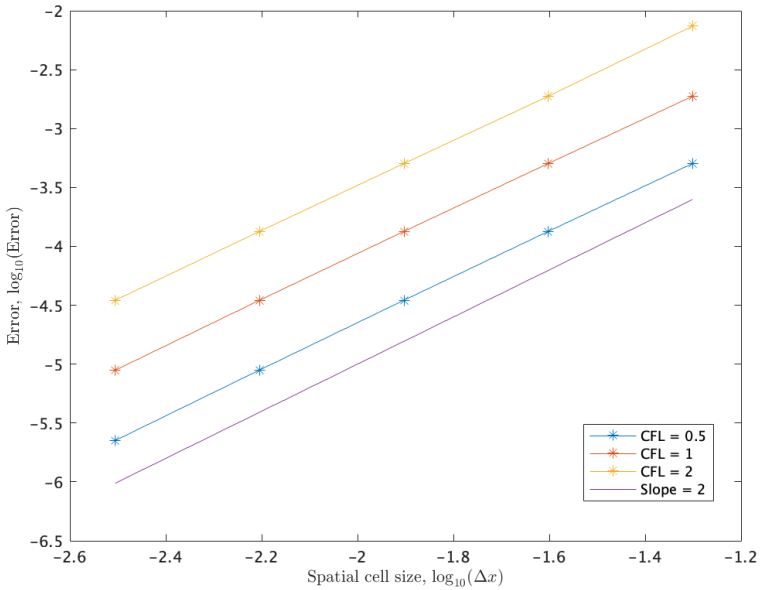

Figure: Inflow Dirichlet $k = 2$

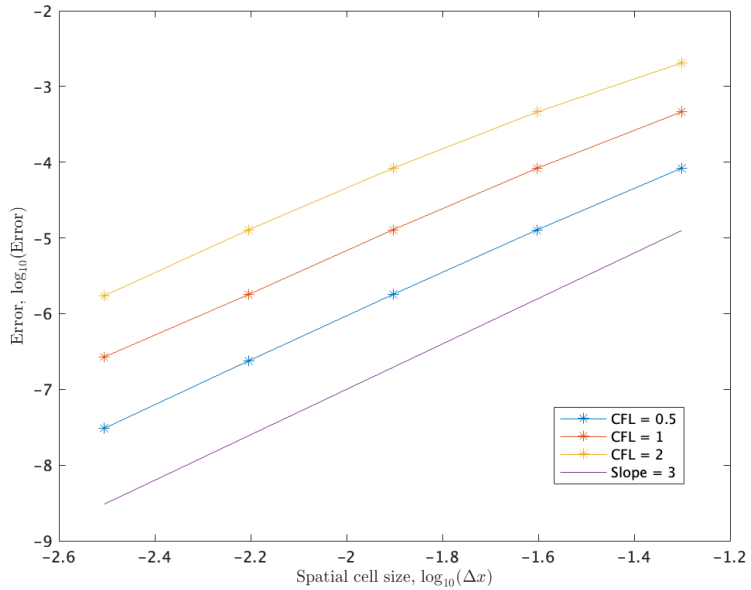

Figure: Inflow Dirichlet $k = 3$

Numerical results: general boundary corrections

As shown in the figure, the use of the k-th partial sum yields k-th order accuracy, thereby verifying our theories. Moreover, the scheme allows for large CFL numbers, say CFL $= 1$ and 2.

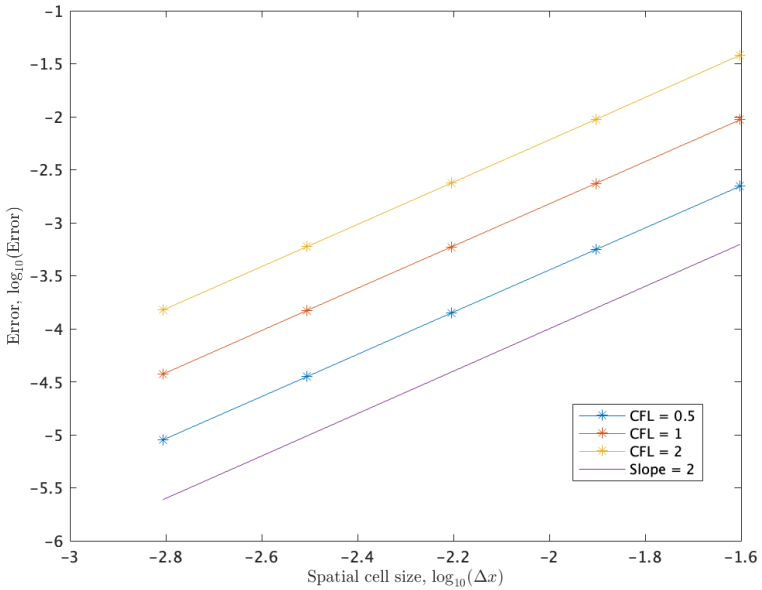

Figure: Neumann $k = 2$

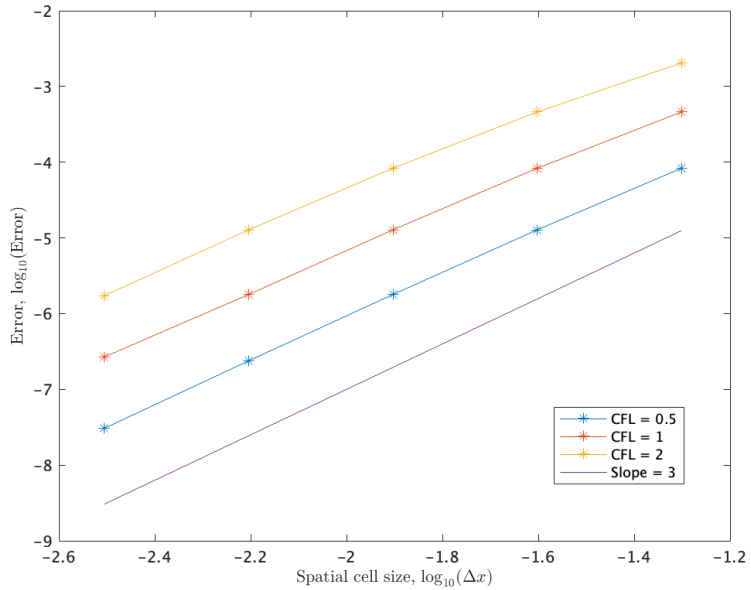

Figure: Neumann $k = 3$

Numerical results: general boundary corrections

Two-dimensional Drumhead Example: The exact solution is given by separation of variables.

$$\begin{cases} u_{tt} = \Delta u, \\ u(x, y, 0) = J_0(k_2\sqrt{x^2 + y^2}), \quad u_t(x, y, 0) = 0, \\ u(\partial\Omega, t) = 0 \end{cases} \tag{21}$$

$$(x, y) \in \Omega := \{(x, y) \in \mathbb{R}^2 : x^2 + y^2 \leq 1\}$$

where k_2 is the second positive zero of Bessel function $J_0(x)$. As long as the spatial resolution is given appropriately, the scheme can accurately capture the wave shape and we also remark here that a large CFL can be chosen to solve the problem, due to the unconditional stability of the method. Our scheme can solve the problem with the expected accuracy/order; (see in A. Christlieb, Gong, and Yang, 2024).

Mesh settings

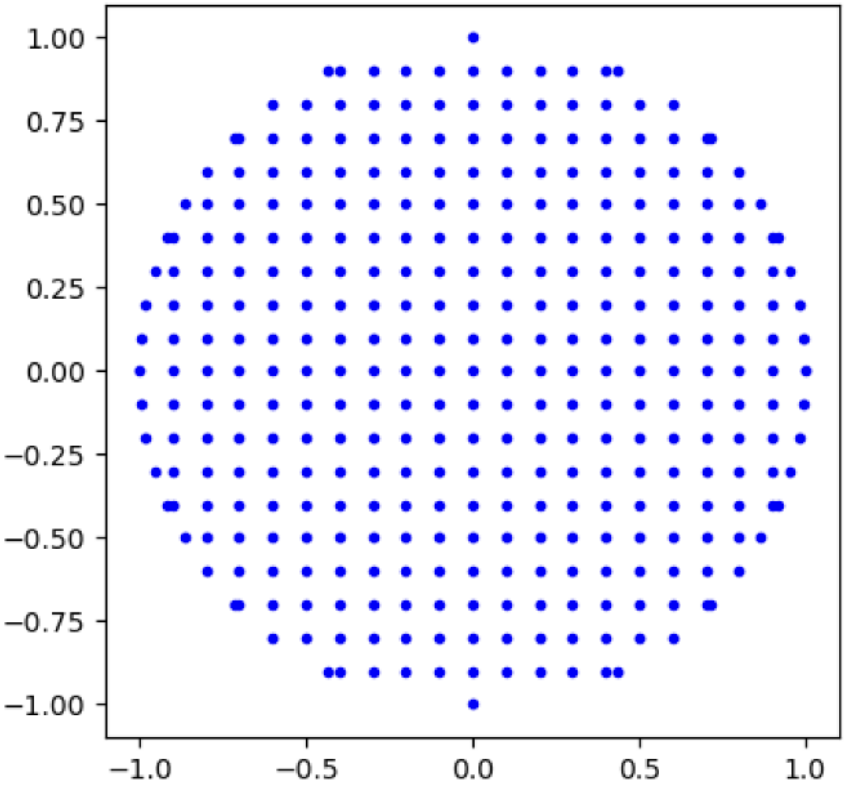

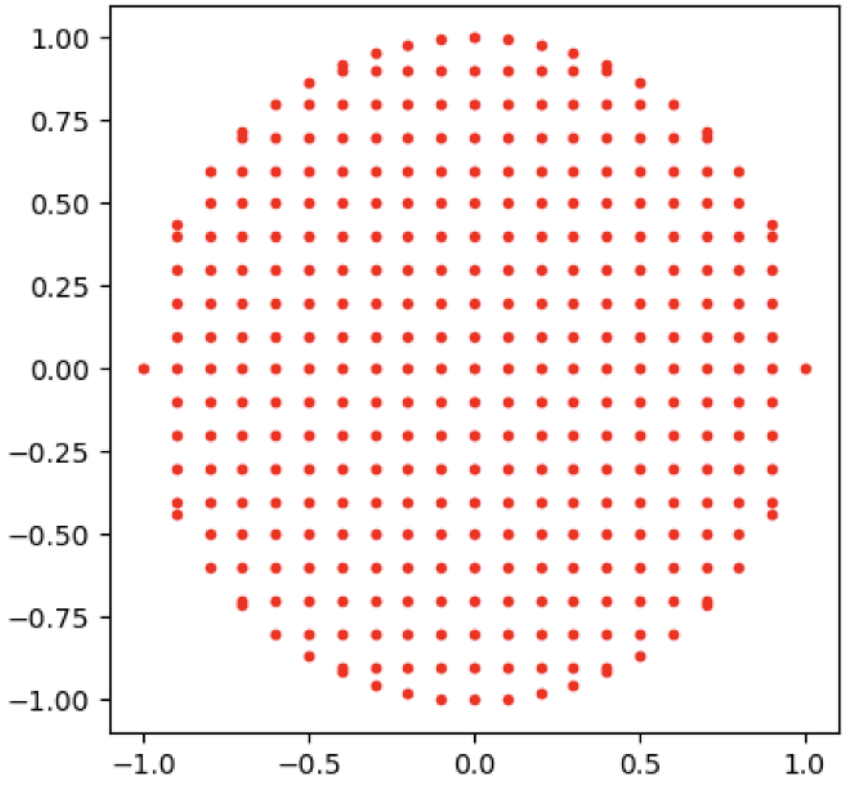

Numerical results: general boundary corrections

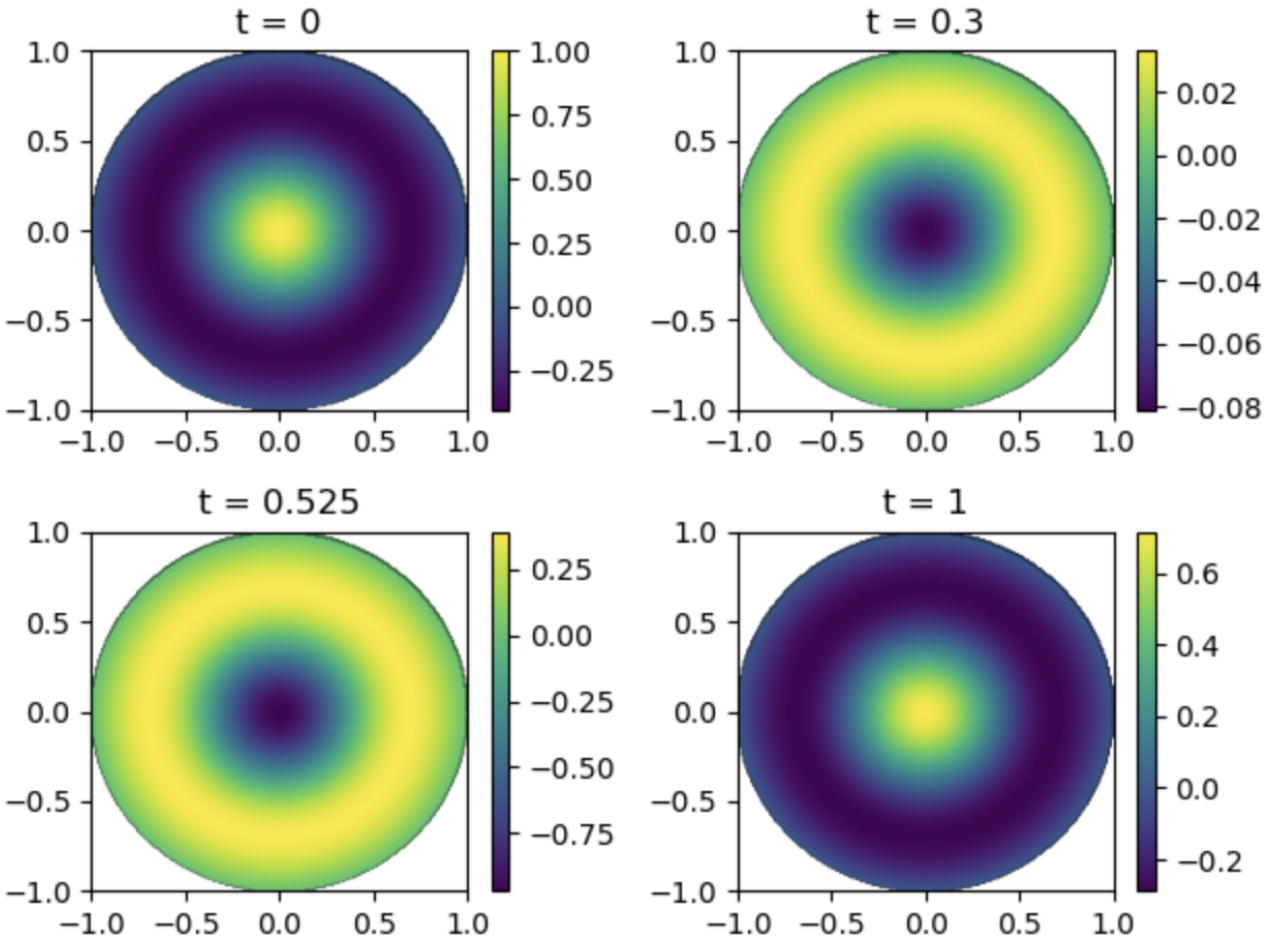

Figure: Numerical solution with different time level with third order scheme for 200×200.

Numerical examples: advection-diffusion

Back to advection-diffusion example:

$$\begin{cases} u_t + c\,u_x = q\,u_{xx}, & -\frac{1}{2} \le x \le \frac{1}{2}, \\ u(x,0) = \sin(\pi x) e^{0.5x}, \end{cases} \tag{22}$$

with the Dirichilet boundary condition $u(-\frac{1}{2}, t) = -e^{-\frac{1}{4}t - \pi^2 t - \frac{1}{4}}$ and $u(\frac{1}{2}, t) = e^{-\frac{1}{4}t - \pi^2 t + \frac{1}{4}}$. Here, $c = q = 1$. This problem has the exact solution $u^e(x,t) = e^{-\frac{1}{4}t - \pi^2 t + \frac{1}{2}x} \sin(\pi x)$. The final time is $T = 0.5$.

Numerical examples: advection-diffusion

CFL	N	$k=1.$		$k=2.$		$k=3.$	
		error	order	error	order	error	order
0.5	20	5.00e-02	–	6.70e-03	–	2.40e-03	–
	40	2.47e-02	1.015	1.85e-03	1.857	4.28e-04	2.491
	80	1.23e-02	1.008	4.81e-04	1.943	6.46e-05	2.726
	160	6.13e-03	1.004	1.21e-04	1.996	8.85e-06	2.868
	320	3.06e-03	1.002	2.97e-05	2.022	1.15e-06	2.944
	640	1.53e-03	1.001	7.28e-06	2.030	1.46e-07	2.975
1	20	1.02e-01	–	2.26e-02	–	1.09e-02	–
	40	5.00e-02	1.029	6.71e-03	1.755	2.41e-03	2.182
	80	2.47e-02	1.015	1.85e-03	1.858	4.28e-04	2.493
	160	1.23e-02	1.008	4.81e-04	1.943	6.47e-05	2.727
	320	6.13e-03	1.004	1.21e-04	1.996	8.86e-06	2.868
	640	3.06e-03	1.002	2.97e-05	2.022	1.15e-06	2.946
2	20	2.12e-01	–	6.98e-02	–	4.20e-02	–
	40	1.02e-01	1.057	2.26e-02	1.625	1.09e-02	1.941
	80	5.00e-02	1.029	6.71e-03	1.755	2.41e-03	2.182
	160	2.47e-02	1.015	1.85e-03	1.858	4.28e-04	2.493
	320	1.23e-02	1.008	4.81e-04	1.943	6.47e-05	2.727
	640	6.13e-03	1.004	1.21e-04	1.996	8.86e-06	2.868

What need to solve and Future Directions

- With general boundary conditions, applying to the equations with boundary derivatives not achievable, especially for stiff problems.

$$u_t + c\, u_x = q\, u_{xx}$$

$$u_t + f(u)_x = g(u)_{xx}$$

  - Inverse Lax-Wendroff with extrapolations? (Lu et al., 2021)
  - Not enough! Additional analysis needed.
- For the cases with stiff source terms, current format seems hard to incorporate.
  - Filtering source terms - not sure if it is crazy.
  - Another MOL^T form?

What need to solve and Future Directions

- A very first version: $\frac{u^{n+1}-u^n}{\Delta t} - c^2 \Delta u^{n+1} = S(u^{n+1})$, use the following form (Cho, 2016)

$$\mathcal{L}^{-1}[u^n + \frac{1}{\alpha} S(u^{n+1})] = u^{n+1}.$$

  - Have done great job in periodic boundary conditions.
    - Including Cahn-Hilliard equations and Allen-Cahn equations.
  - Instead of direct adding the source, kernel-based operator also applies to the source.
  - Boundary conditions! Ideas from our current form?

Takeaways

- This is an ongoing long-term project with some progress in both periodic boundary and non-periodic boundary.
- Periodic boundary:
  - consistence operators allowing for more flexibility
- Non-periodic boundary:
  - Incorporating with stiff/non-stiff source terms
  - Implementation of more complex boundary conditions and geometry.
  - More complex equations.
- High dimensional case with complex domain.

References

- Causley, Matthew F and Andrew J Christlieb (2014). "Higher order A-stable schemes for the wave equation using a successive convolution approach". In: *SIAM Journal on Numerical Analysis* 52.1, pp. 220–235.
- Cho, Hana (2016). *Method of Lines Transpose: High-order schemes for parabolic problems*. Michigan State University.
- Christlieb, Andrew, Sining Gong, and Hyoseon Yang (2024). "Boundary corrections for kernel approximation to differential operators". In: *arXiv preprint arXiv:2410.09332*.
- Christlieb, Andrew, Wei Guo, et al. (2020). "Kernel Based High Order "Explicit" Unconditionally Stable Scheme for Nonlinear Degenerate Advection-Diffusion Equations". In: *Journal of Scientific Computing* 82, p. 52.
- Lu, Jianfang et al. (2021). "An inverse Lax-Wendroff procedure for hyperbolic conservation laws with changing wind direction on the boundary". In: *Journal of Computational Physics* 426, p. 109940.

Thank You!

Appendix

In this section, we present the details about the spatial discretization of $\mathcal{H}[u]$ in (3.11). The proposed algorithm is based on our early work on a high order WENO MOL^T schemes for transport problems. Suppose the domain $[a, b]$ is divided by $N + 1$ uniformly distributed grid points

$$a = x_0 < x_1 < \cdots < x_{N-1} < x_N = b,$$

with the mesh size $\Delta x = \frac{b-a}{N}$. Denote u_i^n as the numerical solution at the spatial location x_i and time level t^n. At each grid point x_i, we further denote $I^*[v, \alpha](x_i)$ as I_i^*, where $*$ can be 0, L and R. Note that the convolution integrals I_i^L and I_i^R satisfy a recursive relation

$$I_i^L = I_{i-1}^L e^{-\alpha_L \Delta x} + J_i^L, \quad i = 1, \ldots, N, \quad I_0^L = 0, \tag{4.1a}$$

$$I_i^R = I_{i+1}^R e^{-\alpha_R \Delta x} + J_i^R, \quad i = 0, \ldots, N-1, \quad I_N^R = 0, \tag{4.1b}$$

respectively, where

$$J_i^L = \alpha_L \int_{x_{i-1}}^{x_i} v(y) e^{-\alpha_L (x_i - y)} dy, \quad J_i^R = \alpha_R \int_{x_i}^{x_{i+1}} v(y) e^{-\alpha_R (y - x_i)} dy. \tag{4.2}$$

Therefore, once we have computed J_i^L and J_i^R for all i, we then can obtain I_i^L and I_i^R via the recursive relation. In addition, the convolution integral $I^0[v, \alpha_0](x)$ can be split into $I^L[v, \alpha_0](x)$ and $I^R[v, \alpha_0](x)$, i.e.,

$$I^0[v, \alpha_0](x) = \frac{1}{2}(I^L[v, \alpha_0](x) + I^R[v, \alpha_0](x)).$$

Appendix

1. As with the standard WENO methodology, we first choose the three small stencils as $S_r(i) = \{x_{i-3+r}, x_{i-2+r}, x_{i-1+r}, x_{i+r}\}$, $r = 0,\ 1,\ 2$. On each small stencil, there is a unique polynomial $p_r(x)$ of degree at most three which interpolates $v(x)$ at the nodes in $S_r(i)$. Then we are able to compute three candidates for J_i^L denoted by $J_{i,r}^L$, $r = 0,\ 1,\ 2$

$$J_{i,r}^L = \alpha \int_{x_{i-1}}^{x_i} e^{-\alpha(x_i - y)} p_r(y) dx = \sum_{j=0}^{3} c_{-3+r+j}^{(r)} v_{i-3+r+j},$$

where the coefficients $c_{-3+r+j}^{(r)}$ depend on α and the cell size Δx, but not on v.

2. On the entire big stencil $S(i) = \{x_{i-3}, \ldots, x_{i+2}\}$, there is a unique polynomial $p(x)$ of degree at most five interpolating $v(x)$ at the nodes in $S(i)$. Then we have

$$J_{i,S}^L = \alpha \int_{x_{i-1}}^{x_i} e^{-\alpha(x_i - y)} p(y) dx = \sum_{j=0}^{5} c_{-3+j} v_{i-3+j} = \sum_{r=0}^{3} d_r J_{i,r}^L \tag{4.3}$$

that approximates J_i^L with the linear weights d_r.

3. Replace the linear weights d_r with the nonlinear weights ω_r that are defined as

$$\omega_r = \frac{\tilde{\omega}_r}{\sum_{s=0}^{2} \tilde{\omega}_s}, \quad \text{with } \tilde{\omega}_r = \frac{d_r}{(\epsilon + SI_r)^2}, \quad r = 0,\ 1,\ 2. \tag{4.4}$$

Appendix

$$\partial_x \approx \frac{\beta}{c\Delta t}\mathcal{D}_L + \frac{\beta}{c\Delta t}\sum_{p=2}^{k}\sigma_{L,i}^{p-1}\mathcal{D}_L^p, \quad \text{and} \quad \partial_x \approx -\frac{\beta}{c\Delta t}\mathcal{D}_R - \frac{\beta}{c\Delta t}\sum_{p=2}^{k}\sigma_{R,i}^{p-1}\mathcal{D}_R^p, \tag{4.5}$$

Remark 5.2 Note that, for the linear advection equation $u_t + cu_x = 0$ with periodic boundary conditions, the third order scheme (Eq. (3.11) with $k = 3$ coupled with third order SSP RK) can only be A(α)-stable. But, fortunately, we find that if the scheme is modified as

$$\begin{aligned}\mathcal{H}[u](x) = &-\frac{\beta}{c\Delta t}\sum_{p=1}^{3}\mathcal{D}_L^p\left[f^+(u), \frac{\beta}{c\Delta t}\right](x) + \frac{\beta}{c\Delta t}\sum_{p=1}^{3}\mathcal{D}_R^p\left[f^-(u), \frac{\beta}{c\Delta t}\right](x)\\ &-\frac{\beta}{q\Delta t}\sum_{p=1}^{3}\mathcal{D}_0^p\left[g(u), \sqrt{\frac{\beta}{q\Delta t}}\right](x)\\ &+\frac{\beta}{c\Delta t}\mathcal{D}_0\left[\mathcal{D}_L^2\left[f^+(u), \frac{\beta}{c\Delta t}\right] - \mathcal{D}_L^2\left[f^-(u), \frac{\beta}{c\Delta t}\right], \frac{\beta}{c\Delta t}\right](x),\end{aligned} \tag{5.4}$$

still with the periodic boundary treatment for the last term, then the scheme coupled with the third order SSP RK integrator is also A-stable provided $0 < \beta \le \beta_{1,3,\max}$. In light of Lemma 3.2, the extra term in (5.4) is in fact an approximation to f_{xxxx}. It will enhance the stability of the scheme and make $\mathcal{H}[u](x)$ fourth order accurate for the case $q \ll c$, i.e., convection dominates. For the homogeneous boundary condition case, we can similarly add the extra term with the treatment (3.13) and make the scheme A-stable. The parameter $\beta_{1,3,\max}$ is given in Table 1.

Appendix

Similar to the previous section, from the linear heat equation

$$\partial_t v - c^2 \partial_{xx} v = 0, \tag{2.19}$$

using the backward Euler time discretization, we obtain

$$(1 - (c^2 \Delta t)\partial_{xx}) v^{n+1} = v^n \tag{2.20}$$

where $v^n := v(t^n)$ and $v^{n+1} := v(t^{n+1})$. We define the operator $\mathcal{L}_0$ as

$$\mathcal{L}_0 = \mathcal{I} - \frac{1}{\alpha^2}\partial_{xx}, \tag{2.21}$$

with $\alpha := \frac{1}{c\sqrt{\Delta t}}$ so that the equation (2.20) can be compactly stated as

$$\mathcal{L}_0[v^{n+1}] = v^n. \tag{2.22}$$

By doing integration by parts twice and we have the numerical solution updated from

$$v^{n+1}(x) = \frac{\alpha}{2}\int_a^b e^{-\alpha|y-x|} v^n(y)dy + \frac{1}{2}(v^{n+1}(b) + \frac{1}{\alpha}v_x^{n+1}(b))e^{-\alpha(b-x)} + \frac{1}{2}(v^{n+1}(a) - \frac{1}{\alpha}v_x^{n+1}(a))e^{-\alpha(x-a)},$$

then we can have the following:

$$v^{n+1}(x) = \frac{\alpha}{2}\int_a^b e^{-\alpha|y-x|} v^n(y)dy + B_0 e^{-\alpha(b-x)} + A_0 e^{-\alpha(x-a)} = I_0[v^n](x) + B_0 e^{-\alpha(b-x)} + A_0 e^{-\alpha(x-a)}, \tag{2.23}$$

where the general boundary operator is:

$$\begin{aligned} B_0 &= \frac{1}{2}(v^{n+1}(b) + \frac{1}{\alpha}v_x^{n+1}(b)) \\ A_0 &= \frac{1}{2}(v^{n+1}(a) - \frac{1}{\alpha}v_x^{n+1}(a)). \end{aligned} \tag{2.24}$$

Appendix

Now depending on the given boundary information we could furthermore provide A_0 and B_0 in different format. For example, for the Dirichlet boundary condition, we have:

$$\begin{aligned} B_0 &= \frac{1}{1-\mu^2}(v^{n+1}(b) - \mu v^{n+1}(a) + \mu I_0[v^n](a) - I_0[v^n](b)) \\ A_0 &= \frac{1}{1-\mu^2}(v^{n+1}(a) - \mu v^{n+1}(b) + \mu I_0[v^n](b) - I_0[v^n](a)), \end{aligned} \tag{2.25}$$

with $\mu = e^{-\alpha(b-a)}$; while for the Neumann boundary condition, we have:

$$\begin{aligned} B_0 &= \frac{1}{\alpha(\mu^2-1)}(\mu v_x^{n+1}(a) - v_x^{n+1}(b) - \mu\alpha I_0[v^n](a) - \alpha I_0[v^n](b)) \\ A_0 &= \frac{1}{\alpha(\mu^2-1)}(v_x^{n+1}(a) - \mu v_x^{n+1}(b) - \mu\alpha I_0[v^n](b) - \alpha I_0[v^n](a)). \end{aligned} \tag{2.26}$$